THE IMPACT OF SMALL SYNCHRONIZATION ERRORS ON EIGENMODE TRANSMISSION

Dominik Schulz[*] *and Martin Haardt*[†]

[*]Communication Networks Research Laboratory
Ilmenau University of Technology
PO Box 100565, 98684 Ilmenau, Germany
phone: +(49) 3677 691156, fax: +(49) 3677 691143
dominik.schulz@tu-ilmenau.de
web: www.tu-ilmenau.de/kn

[†]Communications Research Laboratory
Ilmenau University of Technology
PO Box 100565, 98684 Ilmenau, Germany
phone: +(49) 3677 692613, fax: +(49) 3677 691195
martin.haardt@tu-ilmenau.de
web: www.tu-ilmenau.de/crl

ABSTRACT

Virtual MIMO systems depend on the exact cooperation among the nodes. Since perfect synchronization will never be feasible in practice, the impact of synchronization errors on a virtual MIMO system is an intriguing problem. Hence, we have investigated random synchronization errors that have the order of magnitude of a symbol interval when using eigenmode transmission.

Our closed-form results show that synchronization errors will have an impact on the performance of MIMO systems. In the low SNR regime small imperfections play virtually no role. In contrast to that, in the high SNR regime significant performance losses may be encountered due to the average inter-stream interference.

1. INTRODUCTION

During the last few years MIMO and multi-user MIMO have been the subject of vast interest. However, still not all devices are capable of exploiting the MIMO gains as they are equipped with only a single antenna. In order to let those network nodes exploit MIMO advantages one has to include cooperation among the user terminals (see [8], [1]). This is what is referred to as virtual MIMO. In virtual MIMO systems at least one side of the transmission is a cluster of nodes that cooperate such as if they were one single antenna array. A virtual MIMO transmission basically consists of the three phases depicted in fig. 1. During the first phase the data is diffused from the source node to all nodes of the transmit cluster which will take part in the transmission. The second phase is dedicated to the actual virtual MIMO transmission between the two virtual MIMO clusters. After this has finished, the last phase is performed by distributed data decoding and data forwarding to the receiver node.

Virtual MIMO brings some advantages at the cost of additional practical impairments. The two main impairments are carrier frequency offsets between the nodes of a cluster and imperfect synchronization among the nodes of a cluster. Our analysis is focused on the synchronization problem.

Since nodes suffer from unequal hardware, self-heating, and environmental changes (e.g., temperature change), clocks will never run perfectly synchronized. This problem can be solved via suitable synchronization protocols on the physical layer as well as on higher layers. For the physical layer, multiple synchronization techniques have been proposed to achieve phase synchronization among all nodes of a virtual MIMO cluster. In [2] an SNR gradient algorithm has been proposed that uses a reference tone emitted by the receiver. A very well-known technique is the firefly synchronization as explained in [7]. Firefly synchronization is an application of the coupled oscillator theory. Additionally, there are also blind synchronization techniques (e.g., [6]).

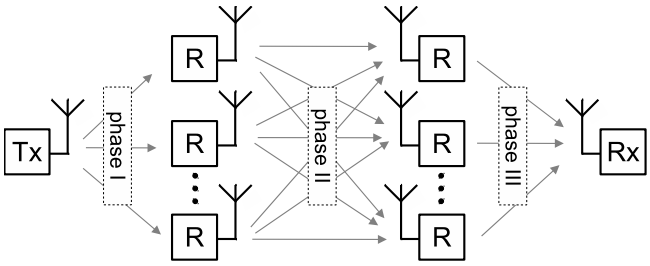

Figure 1: The three phases of a full virtual MIMO transmission – phase I: data diffusion; phase II: virtual MIMO transmission; phase III: data decoding and forwarding

The impairments of imperfect synchronization may be mitigated by suitable channel estimation (see [5]). However, perfect synchronization will never be fulfilled in practice. For that reason Nguen et al. studied this problem in [3]. In contrast to that, we assume in our work that a physical layer synchronization technique is already utilized. Thus we focused on very small synchronization errors that can change randomly. A similar research question has already been investigated in [4] for the case of space-time coding. We have adopted and extended this synchronization error model in our investigations on eigenmode transmission to gain an idea of how imperfectness in synchronization may affect the performance of a virtual MIMO system. Even though eigenmode transmission assumes channel state information at the source nodes it provides a fundamental benchmark of what can be achieved in a virtual MIMO system.

Throughout the whole document we use the following notations: Vectors are indicated by lower-case letters in bold face. Capital letters in bold face refer to matrices. The operators *, $^{\mathrm{T}}$ and $^{\mathrm{H}}$ are used to indicate the complex conjugate, the transpose and the Hermitian transpose of a variable, respectively. In addition to the conventional matrix multiplication we will also use the $\odot$ operator for the Hadamard (element wise) product and the $\otimes$ operator for the Kronecker product. The $\mathrm{vec}(\cdot)$ operator is used to return a vector which has all the columns of the given matrix stacked one below the other. Furthermore the $\mathrm{tr}(\cdot)$ function computes the trace of a matrix, i.e., the sum of its diagonal elements. A diagonal matrix is obtained from a vector via the $\mathrm{diag}(\cdot)$ operator. The expecta-

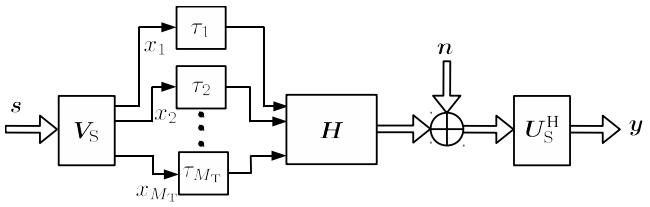

Figure 2: Eigenmode transmission model with imperfect synchronization at transmitter side

tion operator is denoted by $\mathbb{E}\{\cdot\}$.

The rest of the paper is organized as follows: In section 2 we describe the used transmission model and explain the synchronization error model for virtual MIMO nodes. Section 3 derives the SINR values for each substream of a virtual MIMO transmission as well as an upper bound for the overall mutual information. Simulations of the theoretically derived results are presented in section 4. Conclusions and further research issues are given in section 5.

2. SYSTEM MODEL

This section describes the model of transmission and the model of synchronization used throughout the subsequent sections.

Phase differences between the nodes of a virtual MIMO array can be considered as part of the channel. In this case the problem reduces to the conventional channel estimation task. Unfortunately there are types of synchronization problems that may not be treated like this. This problem has already been described in [4] in conjunction with space-time coding. We have adopted this model for our research in order to examine imperfections in synchronization when transmitting via eigenmode transmission.

Our investigations refer to phase II as shown in fig. 1. Assume a set of nodes $\mathcal{N}_T = \{1,\ldots,M_T\}$ and a set of nodes $\mathcal{N}_R = \{1,\ldots,M_R\}$ which form a virtual MIMO array at the transmitter side and at the receiver side, respectively. For the sake of simplicity we will stick to synchronization imperfections only at the transmitter side and assume perfect synchronization among the receive nodes. Note that this model can easily be extended to an imperfectly synchronized virtual MIMO array at the receiver side as well. Fig. 2 shows the corresponding block diagram.

The transmitter uses $g_P(t)$ as the pulse shaping function. The receiver applies a matched filter (MF) to the received signal. Hence after the MF the receiver samples the autocorrelation function $\varphi_{gg}(t)$ of $g_P(t)$. We assume that $\varphi_{gg}(t)$ fulfills the Nyquist inter-symbol interference (ISI) criterion, i.e.,

$$\varphi_{gg}(kT_S) = \begin{cases} 1 & k = 0 \\ 0 & \text{otherwise} \end{cases}, \quad k \in \mathbb{Z}, \tag{1}$$

where T_S is the symbol duration. In a synchronous system (1) states that at time instant n there is no inter-symbol interference from different time slots. Furthermore $\boldsymbol{\tau}[n] := [\tau_1[n] \quad \ldots \quad \tau_{MT}[n]]^T$ is the vector of the random timing errors at time instant n. The elements of $\boldsymbol{\tau}[n]$ are drawn from an arbitrary distribution so that $|\tau_m[n]| \leq \sigma$ and presumed to be mutually independent. This allows us to define the vector

$$\begin{aligned}&\boldsymbol{g}(n,\boldsymbol{\tau}[n])\\ &\quad := [\varphi_{gg}(nT_S - \tau_1[n]) \quad \ldots \quad \varphi_{gg}(nT_S - \tau_{M_T}[n])]^T\end{aligned}$$

Furthermore, we define the diagonal matrix

$$\boldsymbol{G}(n,\boldsymbol{\tau}[n]) := \operatorname{diag}(\boldsymbol{g}(n,\boldsymbol{\tau}[n])).$$

The input-output relation of the discussed Virtual MIMO system at time instant k is given by the following equation.

$$\boldsymbol{y}[k] = \sum_{n=0}^{\infty} \boldsymbol{H}\boldsymbol{G}(n,\boldsymbol{\tau}[k])\boldsymbol{x}[k-n] + \boldsymbol{n}[k] \tag{2}$$

In this equation $\boldsymbol{x}[k] \in \mathbb{C}^{M_T \times 1}$ and $\boldsymbol{y}[k] \in \mathbb{C}^{M_R \times 1}$ are the transmit vector and receive vector, respectively. The channel is assumed to be a flat-fading Rayleigh channel with channel matrix $\boldsymbol{H} \in \mathbb{C}^{M_R \times M_T}$. The additive white Gaussian noise is denoted by the vector $\boldsymbol{n}[k] \in \mathbb{C}^{M_R \times 1}$. Its elements are independent identically distributed with zero mean.

The maximum delay σ is assumed to be much less than a single symbol interval T_S, i.e., $\sigma \ll T_S$ such that

$$\frac{\sum_{n=1}^{\infty} \left|\varphi_{gg}(-nT_S - \tau_m[n])\right|}{\left|\varphi_{gg}(\tau_m[0])\right|} \ll 1, \quad \forall m \in [1, M_T]. \tag{3}$$

As an example, fig. 3 shows the maximum possible delays of a root-raised cosine pulse shape according to (3). Condition (3) states that the interference caused by different time slots is much less than the interference caused by the streams at the same time slot. If this is true, the temporal interference can be neglected and (2) can be simplified as follows.

$$\boldsymbol{y}[k] = \boldsymbol{H}\boldsymbol{G}(0,\boldsymbol{\tau}[k])\boldsymbol{x}[k] + \boldsymbol{n}[k]$$

For notational convenience we drop all indices which leads to (4)

$$\boldsymbol{y} = \boldsymbol{H}\boldsymbol{G}\boldsymbol{x} + \boldsymbol{n}, \tag{4}$$

Where $\boldsymbol{G} := \operatorname{diag}(\boldsymbol{g})$ and $\boldsymbol{g} := \boldsymbol{g}(0,\boldsymbol{\tau}[k]) = [\varphi_{gg}(-\tau_1[k]) \quad \ldots \quad \varphi_{gg}(-\tau_{M_T}[k])]^T$.

The focus of this work is eigenmode transmission. Hence, we make use of the singular value decomposition (SVD) of the channel matrix $\boldsymbol{H} = \boldsymbol{U}\boldsymbol{\Sigma}\boldsymbol{V}^H$. Throughout this document $\boldsymbol{V}$ is the (M_T, M_T)-matrix of right singular vectors, $\boldsymbol{U}$ is the (M_R, M_R)-matrix of left singular vectors and $\boldsymbol{\Sigma}$ is the diagonal (M_R, M_T)-matrix of singular values. We presume $\boldsymbol{H}$ and $\boldsymbol{G}$ to be statistically independent.

When using $\boldsymbol{V}$ as a precoding matrix and $\boldsymbol{U}^H$ as a decoding matrix in conjunction with (4) we obtain the following input-output model.

$$\hat{\boldsymbol{s}} = \sqrt{\tfrac{P}{M_T}}\boldsymbol{U}^H\boldsymbol{H}\boldsymbol{x} + \hat{\boldsymbol{n}} = \sqrt{\tfrac{P}{M_T}}\boldsymbol{\Sigma}\boldsymbol{V}^H\boldsymbol{G}\boldsymbol{V}\boldsymbol{s} + \hat{\boldsymbol{n}} \tag{5}$$

Here P is the overall transmit power radiated by all the transmitting nodes. For our investigations, we did not consider the problem of optimal power loading so far. Hence, waterfilling was not included in the shown model.

3. SYNCHRONIZATION ERROR ANALYSIS

This section explains the analytical derivation of the signal-to-interference-and-noise ratio (SINR) which limits the system performance especially in the high SNR regime. The first subsection shows the derivation of the SINR in the presence of synchronization errors, whereas the second subsection discusses the analytical results.

3.1 Derivation of SINR

Small imperfections in synchronization result in inter-stream interference, which may be seen from the decoded symbol of the i-th substream:

$$\hat{s}_i = \sqrt{\tfrac{P}{M_\mathrm{T}}}\sqrt{\lambda_i}\left(\boldsymbol{v}_i^\mathrm{H}\boldsymbol{G}\boldsymbol{v}_i s_i + \boldsymbol{v}_i^\mathrm{H}\boldsymbol{G}\sum_{\substack{\ell=1\\ \ell\neq i}}^{M_\mathrm{T}}\boldsymbol{v}_\ell s_\ell\right) + n_i \qquad (6)$$

The term $\sqrt{\lambda_i}$ denotes the i-th singular value of $\boldsymbol{H}$. The i-th right singular vector is denoted by $\boldsymbol{v}_i$, i.e. $\boldsymbol{V} = [\boldsymbol{v}_1 \quad \dots \quad \boldsymbol{v}_{M_\mathrm{T}}]$. The channel $\boldsymbol{H}$, the matrix $\boldsymbol{G}$ and the symbols s_i are assumed to be random and mutually independent. As a result, this allows us to express the SINR of the i-th subchannel:

$$\mathrm{SINR}_i = \frac{P_1}{P_2 + \frac{M_\mathrm{T}}{\overline{\lambda}_i \rho}} \qquad (7)$$

Here, ρ is the transmit SNR defined as $\rho := P/N_0$ with N_0 being the noise power. The mean eigenvalue of the i-th subchannel is abbreviated by $\overline{\lambda}_i := \mathbb{E}\{\lambda_i\}$. P_1 is the desired signal power and P_2 is the inter-stream interference power.

$$P_1 := \mathbb{E}\left\{\left|\boldsymbol{v}_i^\mathrm{H}\boldsymbol{G}\boldsymbol{v}_i s_i\right|^2\right\}$$

$$P_2 := \mathbb{E}\left\{\left|\boldsymbol{v}_i^\mathrm{H}\boldsymbol{G}\sum_{\substack{\ell=1\\ \ell\neq i}}^{M_\mathrm{T}}\boldsymbol{v}_\ell s_\ell\right|^2\right\}$$

In the following we will separate the influence of the channel ($\boldsymbol{v}$) and the impact of the synchronization errors ($\boldsymbol{G}$). To this end we consider the desired signal term P_1. The signal power is normalized to one. The derivation for the inter-stream interference term P_2 can be performed in a similar fashion.

At first we apply the $\mathrm{vec}(\cdot)$ operator to P_1.

$$\begin{aligned} P_1 &= \mathbb{E}\left\{|s_i|^2 \cdot \boldsymbol{v}_i^\mathrm{H}\boldsymbol{G}^\mathrm{T}\boldsymbol{v}_i\boldsymbol{v}_i^\mathrm{H}\boldsymbol{G}\boldsymbol{v}_i\right\} \\ &= \mathbb{E}\left\{\mathrm{vec}\left(\boldsymbol{v}_i^\mathrm{H}\boldsymbol{G}^\mathrm{T}\boldsymbol{v}_i\boldsymbol{v}_i^\mathrm{H}\boldsymbol{G}\boldsymbol{v}_i\right)\right\} \end{aligned}$$

When utilizing the rule $\mathrm{vec}\left(\boldsymbol{b}^\mathrm{H}\boldsymbol{A}\boldsymbol{b}\right) = \left(\boldsymbol{b}^\mathrm{T}\otimes\boldsymbol{b}^\mathrm{H}\right)\mathrm{vec}(\boldsymbol{A})$ three times the following expression is obtained.

$$P_1 = \mathbb{E}\left\{\mathrm{tr}\left(\left(\boldsymbol{G}^\mathrm{T}\otimes\boldsymbol{G}^\mathrm{T}\right)\left(\boldsymbol{v}_i^*\otimes\boldsymbol{v}_i\right)\left(\boldsymbol{v}_i^\mathrm{T}\otimes\boldsymbol{v}_i^\mathrm{H}\right)\right)\right\} \qquad (8)$$

By converting the trace operator into the inner product of two $\mathrm{vec}(\cdot)$ operators and by applying the mixed-product property of the Kronecker product (8) becomes:

$$P_1 = \mathbb{E}\left\{\mathrm{vec}^\mathrm{T}\left(\boldsymbol{G}\otimes\boldsymbol{G}\right)\mathrm{vec}\left(\left(\boldsymbol{v}_i^*\boldsymbol{v}_i^\mathrm{T}\right)\otimes\left(\boldsymbol{v}_i\boldsymbol{v}_i^\mathrm{H}\right)\right)\right\} \qquad (9)$$

Recall that the matrix $\boldsymbol{G}$ is defined as a diagonal matrix and does not depend on $\boldsymbol{v}_i$. Hence, it is not necessary to incorporate off-diagonal elements in (9) inside the second $\mathrm{vec}(\cdot)$ operator. Cutting out the diagonal elements in the next equation accounts for this observation.

$$P_1 = \mathbb{E}\left\{\boldsymbol{g}^\mathrm{T}\otimes\boldsymbol{g}^\mathrm{T}\right\}\mathbb{E}\left\{\mathrm{diag}\left(\boldsymbol{v}_i^*\boldsymbol{v}_i^\mathrm{T}\right)\otimes\mathrm{diag}\left(\boldsymbol{v}_i\boldsymbol{v}_i^\mathrm{H}\right)\right\} \qquad (10)$$

We define the vector $\boldsymbol{w}_i := \boldsymbol{v}_i \odot \boldsymbol{v}_i^*$ and the two second order moment matrices $\boldsymbol{R}_{w_i w_i} := \mathbb{E}\left\{\boldsymbol{w}_i\boldsymbol{w}_i^\mathrm{T}\right\}$ and $\boldsymbol{R}_{gg} := \mathbb{E}\left\{\boldsymbol{g}\boldsymbol{g}^\mathrm{T}\right\}$ to obtain a more compact version of (10).

$$P_1 = \mathrm{vec}^\mathrm{T}\left(\boldsymbol{R}_{gg}\right)\mathrm{vec}\left(\boldsymbol{R}_{w_i w_i}\right) \qquad (11)$$

As mentioned above, the derivation for P_2 is very similar. Thus, we skip it here and just give the result. To this end we define the vector $\boldsymbol{u}_i := \boldsymbol{v}_i \odot \sum_{\ell=1,\ell\neq i}^{M_\mathrm{T}}\boldsymbol{v}_\ell$ and its second order moment matrix $\boldsymbol{R}_{u_i u_i} := \mathbb{E}\left\{\boldsymbol{u}_i\boldsymbol{u}_i^\mathrm{H}\right\}$. The P_2 term may thus be expressed as:

$$P_2 = \mathrm{vec}^\mathrm{T}\left(\boldsymbol{R}_{gg}\right)\mathrm{vec}\left(\boldsymbol{R}_{u_i u_i}\right) \qquad (12)$$

The formula for the SINR of the i-th substream is obtained by plugging (11) and (12) into (7):

$$\mathrm{SINR}_i = \frac{\mathrm{vec}^\mathrm{T}\left(\boldsymbol{R}_{gg}\right)\mathrm{vec}\left(\boldsymbol{R}_{w_i w_i}\right)}{\mathrm{vec}^\mathrm{T}\left(\boldsymbol{R}_{gg}\right)\mathrm{vec}\left(\boldsymbol{R}_{u_i u_i}\right) + \frac{M_\mathrm{T}}{\overline{\lambda}_i\rho}} \qquad (13)$$

Moreover, it is possible to write down the overall mutual information

$$I(\rho, \boldsymbol{g}) = \sum_{i=1}^{M_\mathrm{T}}\log_2\left(1+\mathrm{SINR}_i\right) \qquad (14)$$

Regarding (14) it has to be added that this is an upper bound of the achievable mutual information. This is due to the fact that we neglected the inter-symbol interference.

3.2 Discussion

By looking at (13) it is easy to see that in the high SNR regime we obtain a constant signal-to-interference ratio (SIR).

$$\mathrm{SINR}_i = \frac{\mathrm{vec}^\mathrm{T}\left(\boldsymbol{R}_{gg}\right)\mathrm{vec}\left(\boldsymbol{R}_{w_i w_i}\right)}{\mathrm{vec}^\mathrm{T}\left(\boldsymbol{R}_{gg}\right)\mathrm{vec}\left(\boldsymbol{R}_{u_i u_i}\right)} \qquad (15)$$

As a consequence the maximum achievable throughput of a communication system is limited even for high SNR values. This SIR on the one hand depends on the channel via the matrices $\boldsymbol{R}_{w_i w_i}$ and $\boldsymbol{R}_{u_i u_i}$. On the other hand, the SIR depends on the maximum synchronization error σ.

For a given number of transmit antennas and receive antennas the matrices $\boldsymbol{R}_{w_i,w_i}$ and $\boldsymbol{R}_{u_i,u_i}$ are constants if the channel statistics does not change.[1] We consider an extreme case to get some information about $\boldsymbol{R}_{w_i,w_i}$ and $\boldsymbol{R}_{u_i,u_i}$. Suppose a perfectly synchronized transmit array is given or in other words $\boldsymbol{g} = \boldsymbol{1}_{M_\mathrm{T}\times 1}$ is a vector of M_T ones. Hence, $P_1 = 1$ in this case. Consequently we see that

$$\sum_m^{M_\mathrm{T}}\sum_n^{M_\mathrm{T}}\left[\boldsymbol{R}_{w_i,w_i}\right]_{m,n} = 1 \quad .$$

[1] The exact values may be implementation dependent as a result of the scaling ambiguity of the SVD.

The term P_2 vanishes in this case enforcing that the following holds:

$$\sum_{m}^{M_T}\sum_{n}^{M_T}[\boldsymbol{R}_{u_i,u_i}]_{m,n}=0$$

Furthermore, $\boldsymbol{R}_{u_iu_i}$ is symmetric and all diagonal elements are positive.

4. SIMULATIONS

The purpose of this section is to show the performance of eigenmode transmission under inaccurate synchronization conditions. To this end we show the behavior of the individual substreams and the approximate mutual information.

As shown in the previous section synchronization leads to a constant SIR term in the high SNR regime. For our simulations, we chose a root-raised cosine pulse shape. The previous investigations are only valid if (3) holds. We chose the left hand side of (3) to be strictly less than 0.1. Based on that, we numerically computed the maximum allowed synchronization error τ_m. The results are shown in fig. 3. When using a roll-off factor of 0.5 a maximum positive or negative delay of $0.12T_S$ is allowed.

Given this result, we have simulated a system with $M_T = 3$ transmit antennas and $M_R = 4$ receive antennas that employs eigenmode transmission without water pouring. The symbols are chosen from a QPSK constellation and are transmitted over an uncorrelated flat fading Rayleigh channel. Furthermore, the roll-off factor was set to 0.5. The delays τ_m are drawn from a uniform distribution between $-\sigma$ and $+\sigma$.

Fig. 4 shows three different conditions: The first condition assumes perfect synchronization. The second and the third condition assume imperfectly synchronized systems with $\sigma = 0.01T_S$ and $\sigma = 0.1T_S$ respectively.

Perfect synchronization results in a straight line since (13) reduces to the simple SNR term. A synchronization error not larger than one percent of a symbol interval does not effect the system much. However, random delays that may be ten times larger than that show a clear effect in the high SNR regime. The saturation for high SNR values will limit the achievable throughput as shown in fig. 5.

Fig. 6 shows a BER simulation using the same scenario as above. The BER, in contrast to the mutual information, is nearly unaffected in the presence of small synchronization errors.

5. CONCLUSIONS

Synchronization in a distributed MIMO transmission with eigenmode beamforming is a crucial issue. However, imperfections in synchronization are acceptable to a certain extent. We have shown how to compute an upper bound for the achievable mutual information in the unsynchronized case. It turns out that there is an upper limit. Hence increasing the signal power and thus increasing the transmit SNR is not always reasonable depending on the synchronization accuracy.

Further studies are needed to investigate the case of power loading, i.e., waterfilling. The question is whether the conventional power loading is still the optimal one in an unsynchronized case.

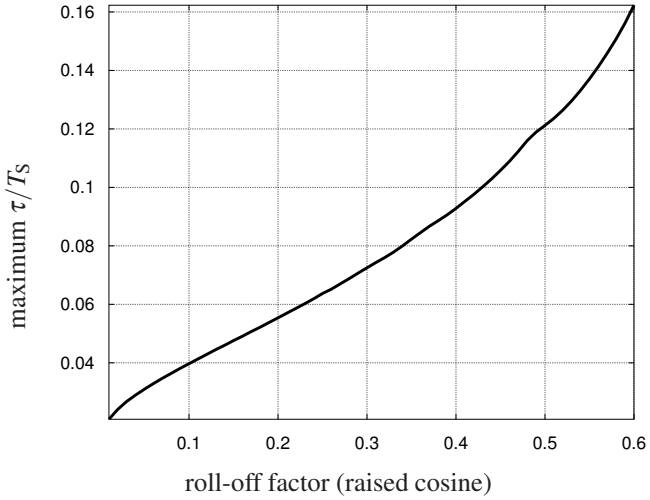

Figure 3: Possible timing errors versus the raised cosine roll-off factor so that the left hand side of (3) is less than 0.1, i.e., temporal inter-symbol interference can be neglected.

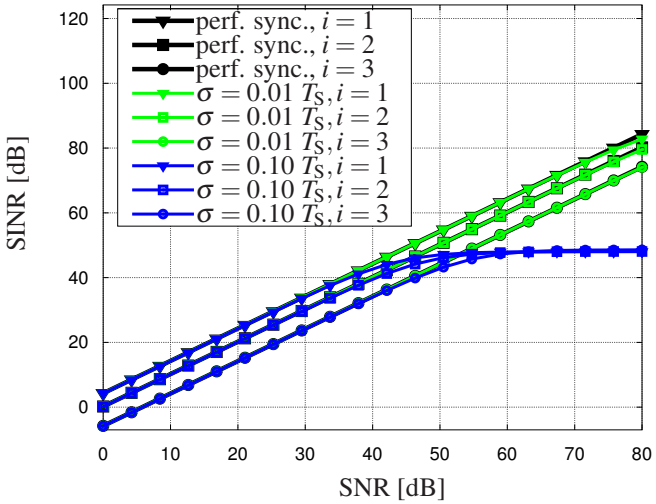

Figure 4: SINR of each i-th substream in a system with $M_T = 3$ and $M_R = 4$ under different synchronization conditions.

The channel properties are reflected via the two second moment matrices. More research on their exact properties is needed.

In distributed communications we do not just encounter synchronization problems. Unknown carrier frequency offsets degrade the system performance as well. This problem should be taken into account in order to obtain a comprehensive model of a distributed communication system.

6. ACKNOWLEDGEMENT

Our research was kindly supported by the International Graduate School on Mobile Communications (Mobicom), which is funded by the German Research Foundation (DFG).

REFERENCES

[1] M. Dohler. *Virtual antenna arrays*. PhD thesis, Kings College London, University of London, 2003.

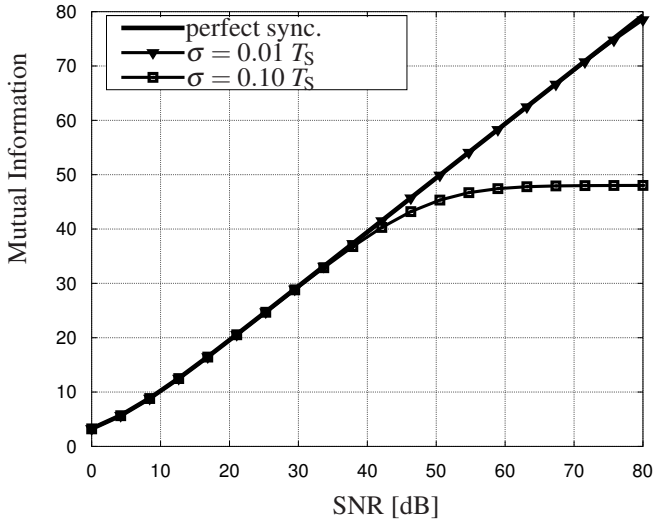

Figure 5: Mutual information in a system with $M_T = 3$ and $M_R = 4$ under different synchronization conditions.

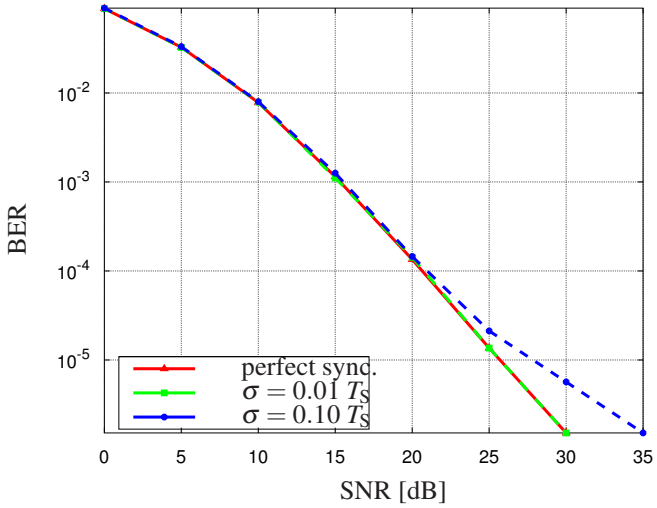

Figure 6: BERs under different synchronization conditions using $M_T = 3$ and $M_R = 4$.

[2] R. Mudumbai, J. Hespanha, U. Madhow, and G. Barriac". Scalable feedback control for distributed beamforming in sensor networks. In *Proc. International Symposium on Information Theory*, pages 137–141, September 2005.

[3] T.-D. Nguyen, O. Berder, and O. Sentieys. Impact of transmission synchronization error and cooperative reception techniques on the performance of cooperative MIMO systems. In *IEEE International Conference on Communications*, pages 4601–4605, 2008.

[4] R. C. Palat, A. Annamalai, and J. H. Reed. Upper bound on bit error rate for time synchronization errors in bandlimited distributed MIMO networks. In *IEEE Wireless Communications and Networking Conference*, pages 2058–2063, 2006.

[5] M. Sichitiu and C. Veerarittiphan. Simple, accurate time synchronization for wireless sensor networks. In *Wireless Communications and Networking 2003*, pages 1266–1273, 2003.

[6] T.-R. Tsai and D.-F. Tseng. Subspace algorithm for blind channel identification and synchronization in single-carrier block transmission systems. *Signal Processing*, 88(2):296–306, 2008.

[7] A. Tyrrell, G. Auer, and C. Bettstetter. Firefly synchronization in ad hoc networks. *MiNEMA*, 2006.

[8] B. Zafar, D. Schulz, S. Gherekhloo, and M. Haardt. Adhoc networking solutions for cooperative MIMO multihop networks. *IEEE Vehicular Technology Magazine*, 6, 2011.